Sustained Wind Forcing and Water Level Anomalies in Annapolis, Maryland

ALEXANDER R. DAVIES,[a] JOSEPH P. SMITH,[a] DAVID S. MANDELL,[b] GEORGE DAVIS,[a] AND FOREST Y. WAN[a]

[a] *Oceanography Department, U.S. Naval Academy, Annapolis, Maryland*
[b] *Office of Emergency Management, City of Annapolis, Annapolis, Maryland*

(Manuscript received 28 May 2021, in final form 18 November 2021)

ABSTRACT: Like many coastal communities throughout the mid-Atlantic region, relative sea level rise and accelerating instances of coastal nuisance flooding are having a tangible negative impact on economic activity and infrastructure in Annapolis, Maryland. The drivers of coastal nuisance flooding, in general, are a superposition of global, regional, and local influences that occur across spatial and temporal scales that determine water levels relative to a coastal datum. Most of the research to date related to coastal flooding has been focused on high-impact episodic events, decomposing the global and regional drivers of sea level rise, or assessing seasonal-to-interannual trends. In this study, we focus specifically on the role of short-duration (hours) meteorological wind forcing on water level anomalies in Annapolis. Annapolis is an ideal location to study these processes because of the orientation of the coast relative to the prevailing wind directions and the long record of reliable data observations. Our results suggest that 3-, 6-, 9-, and 12-h sustained wind forcing significantly influences water level anomalies in Annapolis. Sustained wind forcing out of the northeast, east, southeast, and south is associated with positive water level anomalies, and sustained wind forcing out of the northwest and north is associated with negative water level anomalies. While these observational results suggest a relationship between sustained wind forcing and water level anomalies, a more robust approach is needed to account for other meteorological variables and drivers that occur across a variety of spatial and temporal scales.

SIGNIFICANCE STATEMENT: Coastal nuisance flooding, often the result of positive water level anomalies, is having a negative economic impact in Annapolis, Maryland. Coastal flooding research has primarily focused on high-impact episodic events, trends in sea level rise, or seasonal to interannual variability in flooding. In this study we show that short-duration wind forcing ($\leq$12 h) likely has a significant impact on both positive and negative water level anomalies in Annapolis. While this was empirically known by local stakeholders, in this study we attempt to quantify the relationship. These results could help local stakeholders to mitigate against economic and infrastructure losses resulting from coastal nuisance flooding.

KEYWORDS: Estuaries; Flood events; Sea level; Coastal meteorology

1. Introduction

Throughout the U.S. mid-Atlantic region, relative sea level (RSL) is increasing due to both global mean sea level rise driven by anthropogenic climate change (Merrifield et al. 2009; Church and White 2011; Cazenave and Le Cozannet 2013) and regional dynamics (Boon et al. 2010; Eggleston and Pope 2013; Zervas et al. 2013; Kopp et al. 2015). The long-term trend of RSL in Annapolis, Maryland, located within the Chesapeake Bay, is 3.51 mm yr^{-1} (Sweet et al. 2014) with a near-linear long-term trend in the annually averaged water levels from 1929 through 2019 (Fig. 1; see section 2 for a description of data and methods).

While Fig. 1 indicates an apparent linear trend in RSL rise in Annapolis, recent studies suggest that the mid-Atlantic region is a "hot spot" for accelerating RSL rise over recent decades (Boon 2012; Sallenger et al. 2012; Kopp 2013). One potential cause for the observed acceleration in RSL rise throughout the mid-Atlantic region is Gulf Stream variability (Ezer et al. 2013; Ezer and Atkinson 2014), which is potentially related to changes in the Atlantic meridional overturning circulation associated with climate change (Sallenger et al. 2012; Srokosz et al. 2012; Smeed et al. 2014; Ezer 2015). Future projections (e.g., Parris et al. 2012; Hall et al. 2016) suggest that water levels in Annapolis will likely continue to rise at or above the current near-linear long-term rate.

In addition to being a hot spot for RSL rise, the mid-Atlantic is also a hot spot for an acceleration in coastal nuisance flooding (also known as "sunny-day flooding" or "high-tide flooding") event frequency and duration. Ezer and Atkinson (2014) showed that accelerating RSL rise is correlated with an increased duration of minor flooding events at multiple tide gauges along the U.S. mid-Atlantic coast. Recent studies by Sweet and others (e.g., Sweet et al. 2014; Sweet and Park 2014) show an exponential increase in both the number of flooding days and hours above flood stage in a given year in Annapolis and at other coastal cities throughout the U.S. mid-Atlantic region. Specifically, Sweet and Park (2014) found a factor-of-10 increase in the number of flooding days across the U.S. mid-Atlantic over the last 50 years. Dahl et al. (2017) found a statistically significant increase in the number of annual flooding events at 11 of 52 tide gauges

Corresponding author: Alexander R. Davies, adavies@usna.edu

Earth Interactions is published jointly by the American Meteorological Society, the American Geophysical Union, and the Association of American Geographers.

DOI: 10.1175/EI-D-21-0013.1

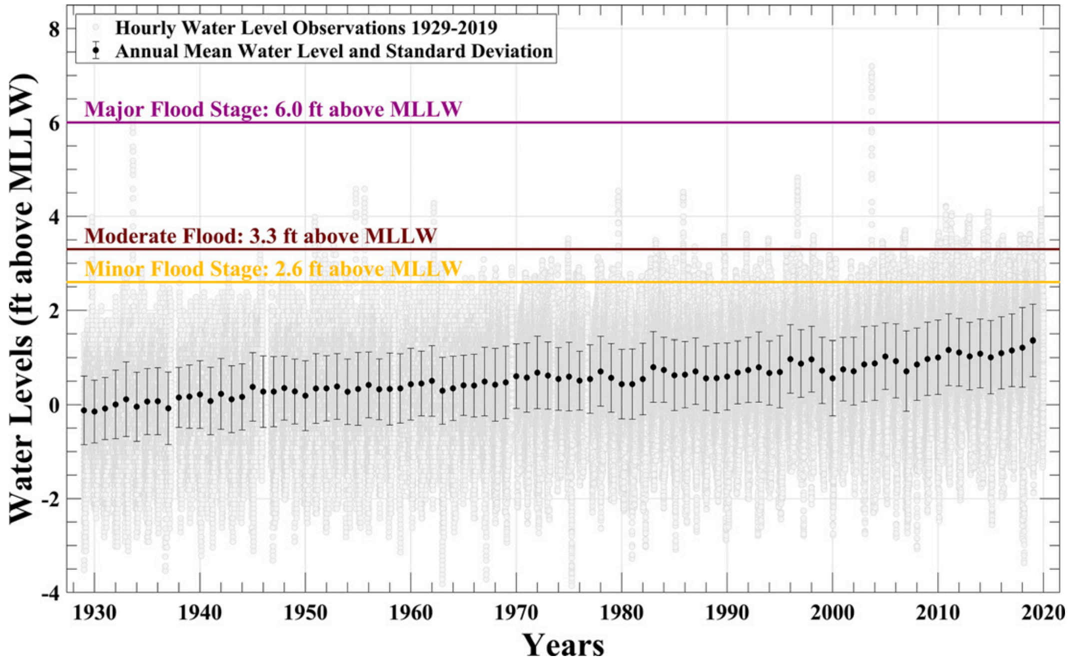

FIG. 1. Annapolis hourly (light gray) and annual mean (black dots with standard deviation) water levels from 1929 to 2019 showing a near-linear rise in sea level. Minor (yellow; 0.79 m), moderate (red; 1.01 m), and major (purple; 1.83 m) flood stages, as defined by the NWS Baltimore/Washington WFO, are plotted.

located on the U.S. East Coast (one being Annapolis) over the 15-yr period from 2001 to 2015.

Annapolis has experienced an exponential increase in hours above flood stage since the middle of the last century (Fig. 2), which is consistent with results from the above-mentioned studies. In the 1930s, water levels exceeded the minor flood stage threshold, defined by the National Oceanic and Atmospheric Administration (NOAA) National Weather Service (NWS) Baltimore/Washington Weather Forecast Office (WFO) to be 2.6 ft (0.79 m) above mean lower low water (MLLW; NOAA 2021), for a total of only 37 h. The number of hours above minor flood stage in Annapolis has

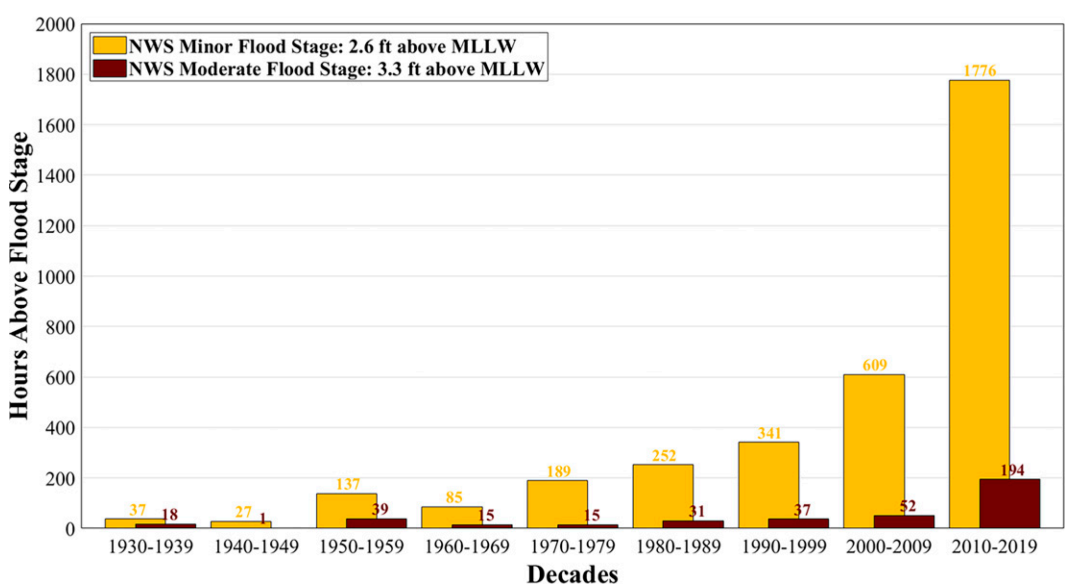

FIG. 2. Hours above flood stage by decade in Annapolis. The number of hourly water level observations in Annapolis above minor (yellow; 0.79 m) and moderate (red; 1.01 m) flood stages by decade, as defined by the NWS Baltimore/Washington WFO.

increased significantly since the 1960s, nearly doubling from the 1990s to the 2000s, and more than doubling between the 2000s and the 2010s, which is indicative of exponential growth (Fig. 2). The hours above moderate flood stage [defined by the NWS Baltimore/Washington WFO to be 3.3 ft (1.01 m) above MLLW (NOAA 2021)] have also accelerated since the turn of the century. During the 2000s, Annapolis experienced 52 hours above moderate flood stage, which is more than any prior decade by ~30%, and this value nearly tripled from the 2000s to 2010s (Fig. 2).

The drivers of coastal nuisance flooding, in general, are a superposition of global, regional, and local influences that occur across spatial and temporal scales that determine local water levels relative to a coastal datum (Sweet et al. 2014). Much of the coastal flooding research to date has been focused on high-impact, episodic events related to storm surge (e.g., McInnes et al. 2002; Sweet and Zervas 2011; Kemp and Horton 2013) or the combination of storm surge, waves, and nontidal residuals (Serafin et al. 2017), decomposing the regional drivers of sea level rise (e.g., Ezer et al. 2013; Miller et al. 2013; Gregory et al. 2013), analyzing seasonal-to-interannual patterns and variability (Ezer 2019; Widlansky et al. 2020), or assessing the longer-term trends in RSL rise (e.g., Sweet et al. 2014; Morris and Renken 2020). However, increasingly common coastal nuisance flooding events occur with regular periodicity and often on different time scales (hours vs days, weeks, months, years, or decades).

A comprehensive understanding of the drivers of coastal nuisance flooding requires, first and foremost, an understanding of the factors that determine water levels, both high and low, relative to the coast on short time scales. On hourly time scales, the relative water level at any point in time is primarily a function of the astronomical tide, which can be estimated by harmonic analysis, and meteorological forcing; lower-amplitude drivers likely also play a role on longer time scales. In this study, we aim to quantify only the meteorological influences on water levels. We therefore assume that the difference between observed hourly water levels and hourly tidal predications represents primarily the meteorological forcing component, which is defined in this study as a water level anomaly (WLA).

Surge from extratropical and tropical storms can result in short-term WLAs (e.g., Zhang and Douglas 2000; Thompson et al. 2013), but they occur sporadically and do not account for the numerous, and increasingly regular, coastal nuisance flooding events. For low-lying areas, heavy precipitation could also be an important contributor to positive WLAs when combined with other factors including wind waves, tidal variability, and surge (Wolf 2009). The co-occurrence of fluvial floods with higher water levels can also contribute to higher WLAs and exacerbate flooding (Ganguli and Merz 2019). Onshore winds likely play an important role in anomalous local water levels (Sweet et al. 2009). Using self-organizing maps, Sheridan et al. (2017) showed that coastal nuisance flooding probabilities and events in five locations along the U.S. East Coast were dependent on the prevailing atmospheric patterns, which in turn, drive the wind field and fetch. It follows that the relationship between directional wind forcing from the prevailing winds and WLAs is dependent on the orientation of the coastline relative to the wind (Cox et al. 2002). In geomorphological complex coastal systems like the Chesapeake Bay and other estuaries, this relationship is not straightforward, especially when complicated by other factors including shallow-water effects and channel convergence (Lyddon et al. 2018).

Annapolis, a hot spot for accelerating instances of coastal nuisance flooding, is an ideal location to study the relationship between directional wind forcing and WLAs because of 1) the orientation of the coastline relative to the prevailing wind directions and 2) the availability of close-proximity water level and meteorological data records (~1 km apart along the Severn River). In this study we identify a relationship between short-duration (hours) directional meteorological wind forcing and WLAs over the period from 2003 to 2019. The results presented here can be used in follow-on studies and modeling approaches to better predict WLAs based on forecast wind speed and direction in Annapolis.

2. Data and methods

Annapolis is home to the U.S. Naval Academy (USNA) and is located at the mouth of the Severn River, a small (~15 km long), brackish tidal tributary of the mesohaline Chesapeake Bay. This bay is a large (>200 km long) partially mixed estuary on the mid-Atlantic coast of the United States. The Chesapeake Bay is generally aligned from south to north (~350°) along its main-stem axis whereas the Severn River is aligned from the southeast to northwest (~315°; Fig. 3). The Severn River subestuary drains a watershed area of ~210 km^2. Freshwater flow in the Severn River is limited to runoff inputs from the numerous small creeks and groundwater-fed streams that empty into the upper section of the river. Physical circulation, especially in the lower estuary, is dominated by tidal exchange with the Chesapeake Bay. The lower estuary is relatively shallow and is urbanized at the mouth where it empties into Annapolis Harbor and the Chesapeake Bay near USNA (Anne Arundel County 2020).

Quality controlled hourly water level observations were downloaded from the NOAA Annapolis tide gauge station (NOAA-8575512; https://tidesandcurrents.noaa.gov/stationhome.html?id=8575512) located on the lower Severn River (Fig. 3). The Annapolis water level data record used spans 1929–2019. Figure 1 shows the hourly water level observations from 1929 through 2019, along with the annual averages and annual standard deviations. Hourly tidal predictions for the Annapolis tide gauge were also downloaded (https://tidesandcurrents.noaa.gov/stationhome.html?id=8575512). Tidal predictions were then matched with coincident water level observations. There were 797 688 hourly tidal predictions (one per hour) from 1 January 1929 through 31 December 2019. However, there were ~5% fewer hourly water level observations over this time span. Hourly WLAs were calculated by subtracting coincident hourly tidal predictions from the hourly water level observations.

Hourly meteorological data (wind speed and wind direction) from 19 December 2002 through 31 December 2019 were recorded by the Automated Surface Observing System

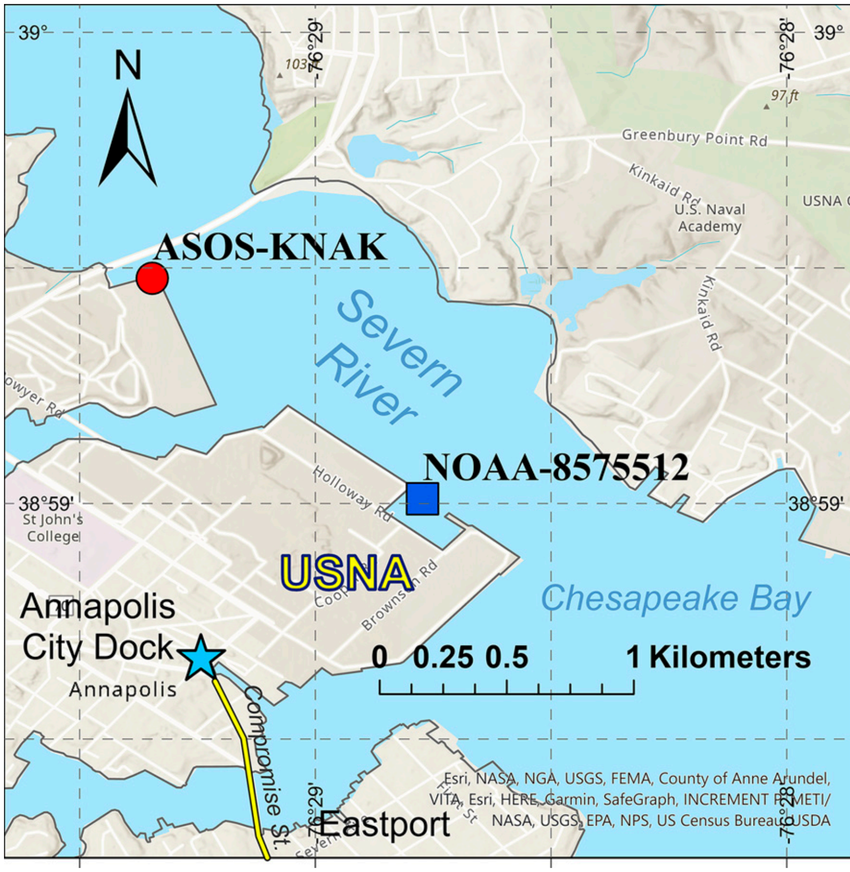

FIG. 3. Map of the mouth of the Severn River in Annapolis, a tidal tributary of the Chesapeake Bay. The locations for the ASOS KNAK weather station (red circle) and the NOAA Annapolis tidal gauging station (NOAA-8575512; blue square) on the grounds of the USNA are shown. The blue star shows the location of Annapolis City Dock, and the yellow line highlights Compromise Street; both are locations prone to recurrent coastal nuisance flooding. The map was created using ESRI ArcGIS Pro, version 2.5.2.

(ASOS) Annapolis (KNAK) weather station. The ASOS-KNAK weather station is located on USNA Hospital Point about 1.2 km up-estuary from the NOAA Annapolis tide gauge station (Fig. 3). A wind rose of the data (Fig. 4) shows that from 2002 to 2019 winds were predominately out of the northwest, south, and southeast in Annapolis. Only regular hourly routine weather reports (METARs) were used in this study, and they were matched with coincident hourly WLAs. The ASOS-KNAK data were downloaded from the Iowa State University Iowa Environmental Mesonet METAR data archive (https://mesonet.agron.iastate.edu). Wind data of less than 2.5 mi h^{-1} (hereinafter mph; 1 mph = 0.447 m s^{-1}), 25 640 total hourly instances, were recorded as calm and not used in our analysis. Note that, as a result of the placement of the ASOS-KNAK station, wind observations from the west-southwest (202.5°–270°) may be partially sheltered by the local terrain.

In this study we investigate sustained (continuous) directional wind forcing over 3, 6-, 9-, and 12-h durations. The criterion used to define sustained directional wind forcing over an n-h period (n = 3, 6, 9, and 12) was that, for a given wind direction observation, all of the $n - 1$ previous wind direction observations must be within ±22.5° of the original directional observation. If this criterion was met, the original wind speed and direction observation was averaged with the $n - 1$ previous wind speed and direction observations. If the sustained directional wind forcing criteria was not met, the data were not considered for analysis. Next the n-hour-averaged sustained wind observations and coincident hourly water level anomalies were binned. The bins used varied by 22.5° and 5 mph. Bins containing three or few data points were discarded and not considered in further analyses.

While the sustained wind periods used in this study (3, 6, 9, and 12 h) are suggestive of atmospheric processes occurring within the mesoscale regime, which is characterized by hourly temporal scales (Orlanksi 1975; Fujita 1981), the prevailing weather patterns and phenomena are likely synoptic scale (days) with winds in near-geostrophic balance away from the frictional boundary layer (Markowski and Richardson 2010). WLAs more clearly fall within the mesoscale regime but are better characterized as being primarily intratidal, which we

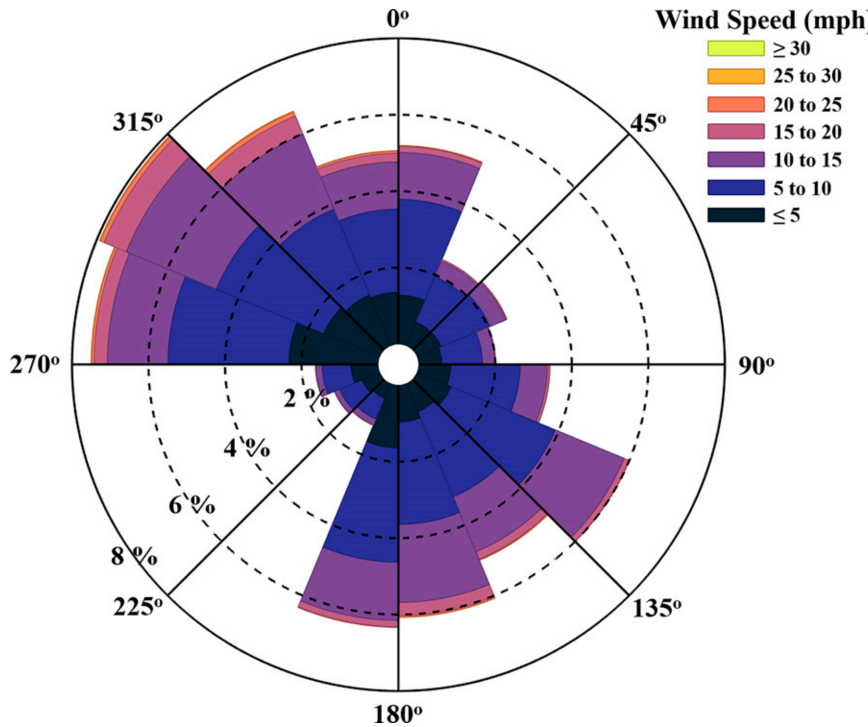

FIG. 4. Wind rose of hourly observations from the ASOS KNAK weather station located on USNA Hospital Point, Annapolis. Data are organized into 45° directional wind bins and 5-mph wind speed bins. The dashed lines indicate the cumulative percent of wind observations.

define as occurring between two subsequent semidiurnal high tides in Annapolis; 3-, 6-, 9-, and 12-h durations for sustained directional wind forcing were chosen to investigate intratidal meteorological forcing. In addition, the percent of occurrence with sustained wind forcing at or above 15 h fell below 5% (additional details are in section 3).

In this study, we have opted to use U.S. Customary Units in our analysis of water levels [i.e., feet (ft)] and wind forcing [i.e., miles per hour (mph)] in lieu of the SI units of meters (m) and meters per second (m s^{-1}), respectively. This unit convention was selected to align with the units typically used by U.S. coastal nuisance flooding stakeholders outside traditional academic and/or research-focused settings. U.S. Customary Units are also used within coastal flooding headlines and alerts issued by the U.S. National Weather Service. Throughout the paper text, the use of U.S. Customary Units for water levels will be accompanied by the corresponding SI unit in parentheses. This paper bins wind speeds in 5-mph increments; the SI conversions are noted here: 5 mph = 2.24 m s^{-1}, 10 mph = 4.47 m s^{-1}, 15 mph = 6.71 m s^{-1}, 20 mph = 8.94 m s^{-1}, 25 mph = 11.18 m s^{-1}, 30 mph = 13.41 m s^{-1}, and 35 mph = 15.65 m s^{-1}, and SI units for wind speed are not used hereinafter.

3. Results

Figure 5 shows the bin-averaged WLAs associated with 3-, 6-, 9-, and 12-h sustained wind forcing, organized circularly by bin-averaged sustained wind speed and direction. Table 1 contains the bin-averaged WLA data plotted in Fig. 5, along with the WLA standard error and number of observations in each bin. In all four circle plots (Figs. 5a–d) the strongest positive hourly WLAs occurred when the sustained directional wind forcing was out of the south (157.5°–202.5°), southeast (112.5°–157.5°) and east (67.5°–112.5°). Meanwhile negative hourly WLAs occurred in all four circle plots (Figs. 5a–d) when the sustained wind forcing was out of the northwest (292.5°–337.5°) except for winds speeds ≤10 mph where the signal is more abstruse.

In total, there were 136 544 data points with coincident meteorological and WLA observations between 19 December 2002 and 31 December 2019. Our analysis found 56 123 instances that satisfied the threshold for sustained directional wind forcing over a duration of 3 h, which represents 41.1% of the record. However, there was an approximate 50% drop off in the number of sustained wind instances for each 3-h increase in sustained wind duration: 6-, 9-, and 12-h sustained directional wind forcing occurred on 25 586, 13 189, and 7 458 instances, representing 18.7%, 9.7%, and 5.5% of the data record, respectively. This result is clearly evident in Fig. 5: the circle sizes (scaled to represent the number of instances of sustained directional wind forcing in a bin) are generally larger in the 3-h sustained wind circle plot (Fig. 5a), with a gradually decreasing number of circles (both large and small) and circle sizes as the duration of sustained wind forcing increased in Figs. 5b–d.

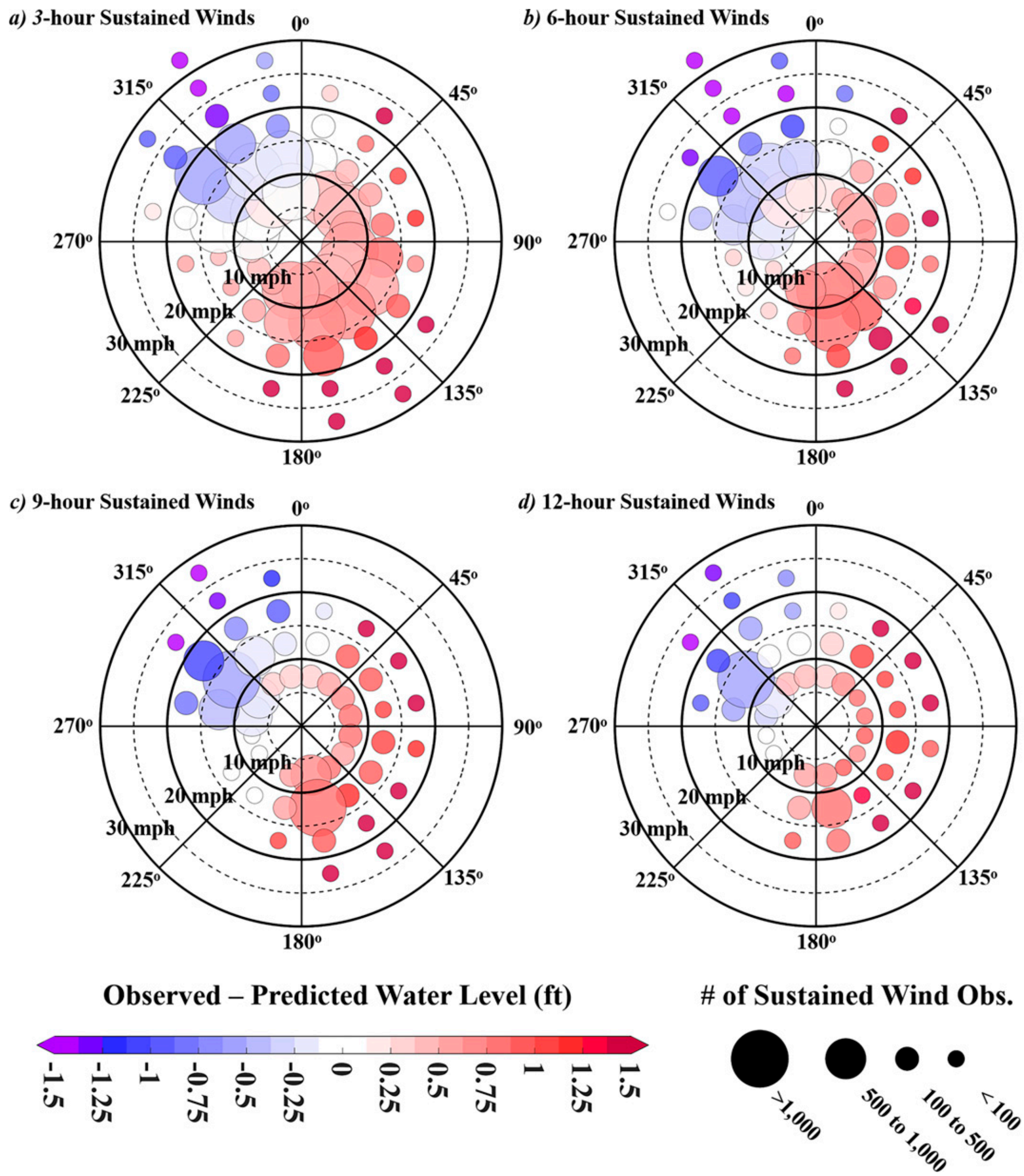

FIG. 5. The impact of sustained wind forcing over (a) 3, (b) 6, (c) 9, and (d) 12 h on WLA (observed − predicted) in Annapolis plotted in wind speed and direction space (bin averaged). Dot color denotes the magnitude of the WLA, and dot size represents the number of observations in a given bin. Red or blue indicates instances in which the WLA is positive or negative, respectively. This figure bins WLAs by increments of 0.25 ft (0.08 m). The bins and their corresponding SI units (in parentheses) are ±0.25 ft (0.08 m), ±0.5 ft (0.15 m), ±0.75 ft (0.23 m), ±1.0 ft (0.31 m), ±1.25 ft (0.38 m), ±1.5 ft (0.46 m).

For 3-h sustained wind forcing, positive WLAs exist between 22.5° and 225° for all three of the lowest wind speed bins (5–10, 10–15, and 15–20 mph; Table 1). The coherence of this result (Fig. 5a), which spans 200° of directional wind forcing, suggests that sustained wind forcing for a duration as little as 3 h out of the east, southeast, and south could result in positive WLAs in Annapolis. Moving to higher-magnitude wind speeds, positive average WLAs greater than 1.5 ft (0.46 m) are present in all four 20–25-mph bins between 112.5° and 202.5° (southeast and south). In addition, there are positive WLAs exceeding 2.0 ft (0.61 m) in the 25–30-mph average wind speed bins between 135° and 180°, although there are limited observations at those higher wind speeds (Table 1). The strongest negative WLAs occurred in the wind direction bin between 315° and 337.5° (Fig. 5a), with average WLA of −1.26 ft (0.38 m) and a standard error of ±0.09 ft (0.03 m), −1.84 ± 0.31 ft (0.56 ± 0.09 m), and −3.25 ± 0.04 ft (0.99 ± 0.01 m) for the 20–25-, 25–30-, and 30–35-mph average wind speed bins, respectively

(Table 1). Sustained wind forcing between 292.5° and 360° resulted in negative WLAs in excess of −0.15 ft (0.05 m) for wind speeds greater than 10 mph. Inside 10 mph, the response to sustained wind forcing out of the northwest (292.5°–337.5°) and north (337.5°–22.5°) is either neutral or weakly positive, suggesting only stronger sustained wind forcing out of those directions drives negative WLAs.

The circle plots of bin-averaged WLAs for 3- and 6-h sustained wind forcing show a similar distribution (Figs. 5a,b), but with an overall reduction in observations (Table 1), which is evident by both smaller and fewer circles in Fig. 5b. However, notable differences did emerge. There are no instances of 6-h sustained wind forcing greater than 25 mph out of the south-southeast in Fig. 5b (135°–180°), which differs from the results in Fig. 5a. In addition, positive WLAs in the 20–25-mph sustained wind speed bins are limited to only the 112.5°–180° bins. While the number of observations in the 15–20-mph bins spanning 45° and 180° decreased between Fig. 5a and Fig. 5b, the bin averaged WLAs notably increased (Table 1), potentially suggesting a more coherent signal. The negative bin-averaged WLAs are similarly evident for 6-h sustained wind speed out of the northwest (Fig. 5b), except with fewer observations in bins greater than 20 mph (Table 1).

For 9-h sustained wind forcing (Fig. 5c) there is a robust signal in the 15–20-mph bins between 22.5° and 202.5° with bin-average positive WLAs ranging over 1.0 ± 0.04 ft (0.30 ± 0.01 m) within the 157.5°–180° bin with 209 observations (Table 1) and 1.91 ± 0.068 ft (0.58 ± 0.02 m) within the 135°–157.5° bin with 70 observations. Similarly, the negative hourly WLA signal remains robust in the northwest quadrant (between 270° and 360°), particularly for wind speeds between 15 and 20 mph (Fig. 5c). Higher sustained wind forcing between 20 and 25 mph resulted in negative WLAs between 292.5° and 360°, all with average negative anomalies in excess of 1.15 ft (0.35 m; Table 1). While only containing six observations, the 315°–337.5° bin with wind forcing between 25 and 30 mph notably features an average negative water level anomaly of −2.09 ± 0.18 ft (−0.64 ± 0.05 m). The 12-h sustained wind forcing circle plot (Fig. 5d) mirrors the 9-h circle plot, with the notable exception being no sustained wind observations in bins above 20 mph associated with positive bin-averaged WLAs.

4. Discussion

Our result suggests that sustained directional wind forcing relative to the geographic orientation of both the Severn River and the Chesapeake Bay plays an important role in driving WLAs in Annapolis. For sections 4a and 4b of this discussion we focus our analysis on 6-h sustained wind forcing (Fig. 5b) but note that the interpretation broadly applies for 3-, 9-, and 12-h sustained directional wind forcing (Figs. 5a,c,d; Table 1).

a. Sustained wind forcing and WLAs relative to the orientation of the Severn River

The Severn River is oriented in a northwest–southeast direction (Fig. 6), which directly aligns with two of the prevailing wind directions in Annapolis (Fig. 4). Negative WLAs associated with sustained wind forcing greater than 10 mph out of the northwest (292.5°–337.5°; Fig. 5b; Table 1) align with the orientation of the Severn River (Fig. 6). We interpret this result as water being blown out of the Severn River basin, resulting in negative WLAs. Overall, 33.7% of all bin-average WLAs (both positive and negative) associated with 6-h sustained wind forcing are out of the northwest (Table 2), and 55.3% of all negative 6-h WLAs are associated with sustained wind forcing out of the northwest. Here we define the threshold for positive and negative WLAs as being ±0.125 ft (±0.04 m), which is approximately 2 times the sampling error of the NOAA Annapolis tide gauge (±0.02 m; NOAA 2020) and the minimum color threshold used in Fig. 5.

While the axis of the Severn River is oriented in a northwest–southeast direction, the mouth of the Severn River widens, allowing for wind forcing out of the northeast, east, and southeast (22.5°–157.5°), as shown in Fig. 6. We note that the compass in Fig. 6 is centered on Annapolis and not the mouth of the Severn River, which would more apparently show the importance of northeast wind forcing. Positive WLAs for all wind speed bins with sufficient data are associated with sustained wind forcing out of the northeast, east, and southeast directions (Fig. 5b; Table 1). The highest overall bin-averaged positive WLA for 6 h of sustained wind forcing was 2.62 ± 0.145 ft (0.8 ± 0.04 m) for 20–25-mph sustained winds out of 135°–157.5°. The highest bin-average WLA associated with 15–20-mph sustained wind forcing was also out of 135°–157.5°, which aligns with the axis of the Severn River. We interpret these results to indicate that positive WLAs occur when sustained wind forcing blows water into the mouth and/or up the axis of the Severn River. These wind directions (northeast, east, and southeast) cumulatively make up 21.3% of all bin-average WLAs (both positive and negative) associated with 6-h sustained wind forcing (Table 2), and 34.3% of all positive WLAs for 6 h of sustained wind forcing.

b. Sustained wind forcing and WLAs relative to the orientation of the Chesapeake Bay

The axis of the main stem of the Chesapeake Bay is oriented nearly north to south from the mouth of the Patapsco River (Baltimore, Maryland) to the mouth of the Patuxent River (Solomons, Maryland, and Patuxent Naval Air Station), which spans a distance of approximately 100 km. Winds from the south (157.5°–202.5°) align with the axis of the main stem of the Chesapeake Bay (Fig. 6) and are also associated with positive bin-average WLAs (Fig. 5b; Table 1). Unlike meteorological forcing directly into the mouth of the Severn River, we interpret this result from a conservation of mass perspective in that southerly winds push water up the spine of the main stem of the Chesapeake Bay, which then inundates smaller tributaries throughout, resulting in positive WLAs. With Annapolis near the mouth of the Severn, it reasons that sustained southerly flow drives positive WLAs. We found that 20.2% of all the bin-average WLAs associated with 6-h sustained wind forcing come from this direction (Table 2), which is nearly as much as the northeast, east, and southeast (22.5°–157.5°)

TABLE 1. Average (Avg) and standard error (Std err) in feet (1 ft = 0.3 m), along with number of observations (No. obs), for WLAs in each wind speed and direction bin. See Fig. 5 for a graphical representation of these data. Only wind bins with data in at least one sustained wind regime are shown. Bins with less than four data points were not considered for this analysis. Std err is calculated as the standard deviation of the data within a bin divided by the square root of the number of observations in a given bin.

	3 h			6 h			9 h			12 h		
Speed	Avg	No. obs	Std err	Avg	No. obs	Std err	Avg	No. obs	Std err	Avg	No. obs	Std err
0°–22.5°												
5–10	0.18	1796	0.013	0.20	744	0.019	0.26	354	0.028	0.33	173	0.039
10–15	0.08	853	0.021	0.04	531	0.026	0.11	319	0.031	0.32	192	0.037
15–20	−0.06	137	0.085	−0.12	89	0.106	−0.24	56	0.139	0.18	35	0.142
20–25	0.26	11	0.152	−0.78	10	0.113	—	0	—	—	3	—
22.5°–45°												
5–10	0.39	1318	0.015	0.51	465	0.025	0.59	218	0.037	0.67	104	0.051
10–15	0.45	491	0.032	0.61	291	0.042	0.89	192	0.045	1.12	137	0.059
15–20	0.81	67	0.100	1.20	49	0.084	1.64	38	0.129	1.91	32	0.222
20–25	1.83	6	0.047	2.02	4	0.199	—	3	—	—	0	—
45°–67.5°												
5–10	0.49	1327	0.015	0.59	529	0.022	0.74	184	0.037	0.85	90	0.052
10–15	0.58	366	0.032	0.75	197	0.046	0.88	113	0.060	1.12	80	0.080
15–20	1.03	38	0.090	1.21	23	0.096	1.66	13	0.136	1.71	6	0.059
67.5°–90°												
5–10	0.57	747	0.018	0.72	261	0.029	0.83	108	0.050	0.86	36	0.099
10–15	0.75	286	0.032	0.87	189	0.041	1.10	92	0.069	1.09	51	0.092
15–20	1.25	23	0.130	1.52	17	0.121	1.73	10	0.030	1.73	8	0.046
90°–112.5°												
5–10	0.59	1042	0.015	0.75	323	0.024	0.85	113	0.036	0.97	37	0.059
10–15	0.77	509	0.020	0.92	295	0.026	1.10	170	0.033	1.24	105	0.051
15–20	0.73	60	0.079	0.81	33	0.095	1.20	15	0.164	0.95	4	0.129
112.5°–135°												
5–10	0.44	3293	0.008	0.52	943	0.015	0.59	219	0.033	0.65	56	0.063
10–15	0.51	1643	0.011	0.69	428	0.024	0.98	103	0.052	1.08	32	0.084
15–20	0.98	101	0.050	1.26	37	0.081	1.46	21	0.136	1.82	6	0.162
20–25	1.82	13	0.120	2.17	4	0.245	—	0	—	—	0	—
135°–157.5°												
5–10	0.49	2216	0.010	0.63	648	0.019	0.79	140	0.037	0.88	51	0.058
10–15	0.65	1411	0.015	0.88	518	0.024	1.18	187	0.039	1.30	78	0.054
15–20	1.14	247	0.040	1.62	114	0.058	1.91	70	0.068	1.69	45	0.067
20–25	2.21	25	0.130	2.62	18	0.145	2.56	7	0.164	—	3	—
25–30	2.67	6	0.096	—	0	—	—	0	—	—	0	—
157.5°–180°												
5–10	0.58	3370	0.008	0.63	1737	0.011	0.65	849	0.015	0.63	375	0.020
10–15	0.74	2794	0.009	0.83	1931	0.011	0.86	1195	0.013	0.82	700	0.018
15–20	0.97	531	0.028	1.08	381	0.033	1	209	0.040	0.85	114	0.059
20–25	1.79	35	0.122	2.09	24	0.133	1.78	10	0.193	—	2	—
25–30	2.23	4	0.321	—	1	—	—	0	—	—	0	—
180°–202.5°												
5–10	0.56	2006	0.011	0.63	801	0.016	0.59	311	0.023	0.54	118	0.032
10–15	0.61	850	0.017	0.65	402	0.023	0.59	218	0.026	0.53	137	0.030
15–20	0.76	106	0.057	0.81	47	0.106	1.02	19	0.157	0.96	8	0.119
20–25	1.51	7	0.120	—	2	—	—	0	—	—	0	—
202.5°–225°												
5–10	0.51	346	0.024	0.48	36	0.074	—	3	—	—	1	—
10–15	0.57	108	0.043	0.29	31	0.068	0.04	7	0.180	—	1	—
15–20	0.50	6	0.132	—	1	—	—	0	—	—	0	—
225°–247.5°												
5–10	0.40	335	0.025	0.30	54	0.049	0.11	9	0.121	0.02	4	0.009
10–15	0.53	73	0.080	0.16	15	0.115	–	5	–	–	2	–
247.5°–270°												
5–10	0.29	351	0.033	0.23	78	0.059	0.05	24	0.101	0.10	8	0.144
10–15	0.46	88	0.068	0.32	21	0.103	—	1	—	—	0	—
15–20	0.57	7	0.277	—	2	—	—	0	—	—	0	—

TABLE 1. (*Continued*)

Speed	3 h Avg	3 h No. obs	3 h Std err	6 h Avg	6 h No. obs	6 h Std err	9 h Avg	9 h No. obs	9 h Std err	12 h Avg	12 h No. obs	12 h Std err
270°–292.5°												
5–10	−0.05	2441	0.014	−0.13	1277	0.018	−0.21	630	0.025	−0.31	270	0.039
10–15	−0.04	1188	0.024	−0.26	896	0.023	−0.48	666	0.022	−0.62	469	0.026
15–20	−0.07	289	0.042	−0.46	216	0.039	−0.78	154	0.044	−0.93	99	0.054
20–25	0.13	31	0.144	0.09	8	0.487	—	2	—	—	0	—
292.5°–315°												
5–10	−0.03	3996	0.011	−0.15	1861	0.015	−0.20	971	0.019	−0.21	541	0.026
10–15	−0.29	3595	0.013	−0.47	2499	0.014	−0.55	1871	0.016	−0.56	1359	0.018
15–20	−0.52	1031	0.026	−0.95	793	0.027	−1.10	598	0.029	−1.06	428	0.032
20–25	−0.88	149	0.078	−1.32	93	0.105	−1.77	59	0.159	−2.14	38	0.109
25–30	−0.91	8	0.426	—	1	—	—	0	—	—	0	—
315°–337.5°												
5–10	0.13	2730	0.011	0.15	1066	0.017	0.27	395	0.028	0.40	162	0.050
10–15	−0.15	2481	0.013	−0.27	1548	0.016	−0.19	807	0.023	0.01	459	0.032
15–20	−0.54	693	0.030	−0.78	438	0.036	−0.66	278	0.047	−0.51	184	0.061
20–25	−1.26	128	0.094	−1.55	82	0.103	−1.33	60	0.129	−1.01	44	0.139
25–30	−1.84	14	0.310	−3.06	4	0.146	−2.09	6	0.179	−1.36	8	0.098
30–35	−3.25	5	0.044	−3.50	5	0.029	—	2	—	—	0	—
337.5°–360°												
5–10	0.11	2031	0.012	0.14	929	0.018	0.28	401	0.030	0.44	167	0.048
10–15	−0.16	1116	0.019	−0.30	735	0.024	−0.23	435	0.032	−0.06	275	0.047
15–20	−0.68	226	0.048	−1.09	162	0.041	−1.00	106	0.055	−0.55	71	0.070
20–25	−0.86	38	0.106	−1.42	24	0.061	−1.15	23	0.092	−0.66	7	0.228
25–30	−0.59	4	0.079	−0.89	4	0.163	—	0	—	—	0	—

combined. Furthermore, 34% of all positive 6-h WLAs are out of the south, meaning WLAs occur as frequently as they do from the northeast, east, and southeast combined.

Winds from the north (337.5°–22.5°) also align with the axis of the main stem of the Chesapeake Bay (Fig. 6) and are associated with negative bin-average WLAs, particularly within the 337.5°–360° directional bin (Fig. 5b; Table 1). We again interpret this result from a conservation of mass perspective. Northerly flow pushes water down the axis of the main stem of the Chesapeake Bay, which, by conservation of mass, drains smaller tributaries resulting in negative WLAs; 13.6% of all the bin-average WLAs associated with 6-h sustained wind forcing come from this direction (Table 2), which is the third highest frequency. In addition, the second highest frequency of negative WLAs (18%; Table 2) is out of the north, making it an important sustained wind direction.

c. Analysis and data limitations

The coherent patterns of positive and negative WLAs associated with sustained wind forcing relative to the orientation of the Severn River and/or Chesapeake Bay inspires confidence in our overall observational results, particularly at sustained wind speeds greater than 10 mph. However, the negative WLAs pattern does not hold for the lowest wind speed bins (5–10 mph; Fig. 5). Weak positive or neutral WLAs are evident throughout the fourth quadrant in the 5–10-mph bins associated with 3 h of sustained wind forcing. While negative WLAs occurred between 270° and 315° in the lowest wind speed bin associated with 6-, 9-, and 12-h sustained wind forcing, positive WLAs were observed for all three of these wind regimes between 315° and 360°. One likely reason is that 5–10-mph sustained winds might not be sufficiently strong enough to have a tangible impact on WLAs, particularly in the 3-h sustained wind regime. While our results suggest that as few as 3 h of sustained wind forcing may have an impact on WLAs, the starting water level and inertial state of the system are also important. Meteorological conditions can change quickly (e.g., frontal passage), which could result in an instantaneous shift in the wind forcing but a lagged water level response. This is evident throughout Fig. 5, with the brightest blue and red colors generally occurring in the 15-mph+ bins as compared with the lower–wind speed bins.

In addition, the WLA record in this study is likely biased positive because the reference tidal prediction data are based on the most recent tidal datum analysis period (1983 through 2001, centered at 1992). Sea level rise is occurring at a rate of 3.51 mm yr^{-1} (Sweet et al. 2014) and, therefore, when considering water level anomalies with respect to tidal predictions, sea level rise likely needs to be incorporated in future analyses. Figure 7 shows an increase in the annual mean WLAs between 2003 and 2020 that approximately paces with the linear rate of RSL rise. This could result in biasing of the WLAs in all quadrants and bins, but the signal is likely more evident in bins where the wind forcing is not as strong (e.g., 5–10-mph bins in Fig. 5). As an example of this, hours where calm winds were observed (see section 2) were omitted from this study, however the mean WLA during those times was 0.31 ft

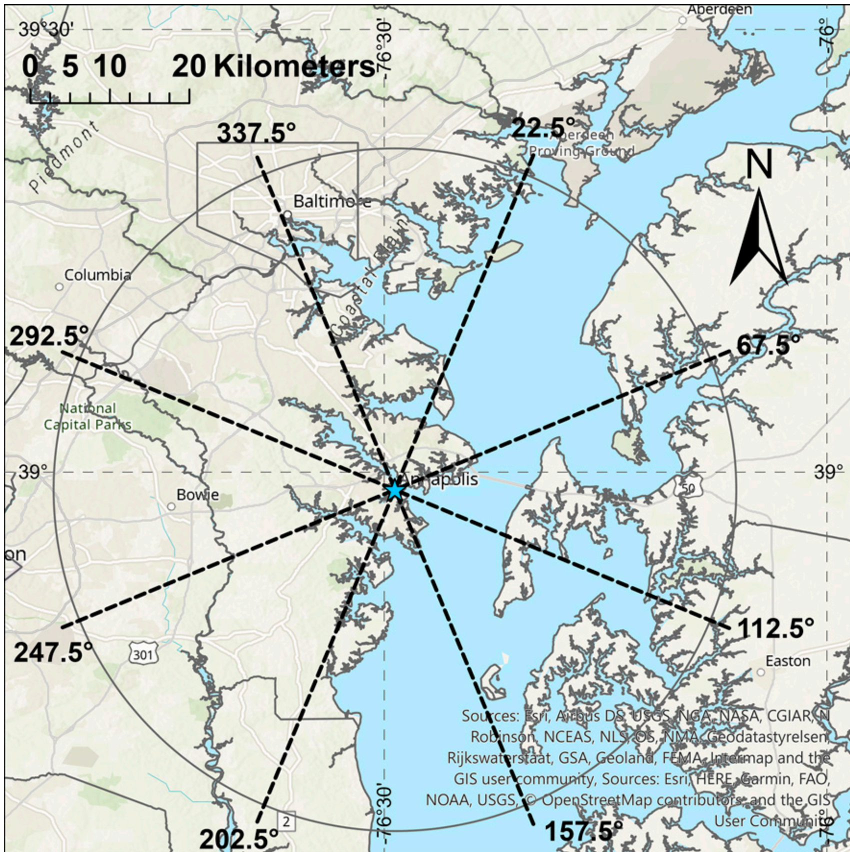

FIG. 6. Directional compass centered over Annapolis. The eight directional bins are set so that the cardinal directions (north, northeast, east, southeast, south, southwest, west, and northwest) are centered in each ±22.5°.

(0.09 m). This emphasizes the need for follow-on studies to better account for the starting water level and inertial state of the system, particularly when wind forcing is weak (as noted in the paragraph above), and to correct for any bias in WLA calculations due to RSL rise. A better method for future studies would be to consider short-duration temporal changes in water level anomalies (e.g., 3-, 6-, 9-, and 12-h differences in WLAs), instead of the WLAs themselves. This could also effectively neutralize the impacts of longer-duration water level drivers that are not considered in this study.

d. *Implications and future work*

Our analysis also revealed that the annually averaged daily standard deviation of water levels has increased by ~10% since the beginning of the 1930s (Fig. 8). For this calculation, we calculated the standard deviation of the hourly water levels on each day and averaged all daily standard deviations over the course of one year. This analysis suggests that in addition to RSL rise and intra-annual or interseasonal variability, the processes driving hour-to-hour water level variability may also be changing. Flick et al. (2003) similarly found that the mean range of the tide (Hicks et al. 2000) increased at a rate of 0.19 ft yr^{-1} (0.06 m yr^{-1}) in Annapolis between 1929 and 1999. Sweet and Park (2014) suggested that even a linear rise in RSL could result in an exponential increase in nuisance flooding, which is often a result of positive WLAs. This highlights the need to understand the short-duration drivers of coastal nuisance flooding.

A robust understanding of the short temporal scale processes driving WLAs is important for forecasters and local stakeholders, including government officials, business owners, and concerned residents who rely on accurate information to mitigate the impacts associated with WLAs and coastal nuisance flooding. Coastal flooding and positive WLAs are already having a measurable impact in downtown Annapolis, and other coastal or estuarine communities. Moderate coastal flooding inundates Compromise Street (Fig. 3), an evacuation route that is adjacent to City Dock in downtown Annapolis and one of only two roadways that accesses the Eastport Peninsula. The Annapolis Office of Emergency Management (OEM) therefore considers coastal flooding to be a life-safety issue given that flooding could impede the capability to evacuate quickly, if necessary. Once water levels exceed approximately 3.0 ft (0.91 m) above MLLW, accessibility to City Dock in downtown Annapolis (Fig. 3) becomes limited, which prompts action from Annapolis OEM related to

TABLE 2. The number of WLAs within a directional bin for the sustained wind regime (No. of WLAs), the percent of the total WLAs within the sustained wind regime that are in the directional bin (% of total WLAs), the number of positive (+) or negative (−) WLAs within a directional bin for the sustained wind regime (No. of ±WLAs), the percent of the total positive or negative WLAs within the sustained wind regime in the directional bin (% of total ±WLAs), percent of WLAs within a directional bin that are positive or negative (% of bin WLAs), and the percent of positive or negative WLAs in a bin relative to all WLAs for the sustained wind regime (% of total WLAs). For this table, only WLAs greater than 0.125 ft (0.04 m) or less than −0.125 ft (−0.04 m) are considered.

Bins		Total WLAs in bin		Positive WLAs in bin				Negative WLAs in bin			
Direction	Bin (°)	No. of WLAs	% of total WLAs	No. of +WLAs	% of total +WLAs	% of bin WLAs	% of total WLAs	No. of −WLAs	% of total −WLAs	% of bin WLAs	% of total WLAs
3-h sustained wind forcing											
North	337.5–22.5	6485	12.4	2976	9.3	45.9	5.7	3509	17.2	54.1	6.7
Northeast	22.5–67.5	3922	7.5	2856	8.9	72.8	5.5	1066	5.2	27.2	2.0
East	67.5–112.5	2752	5.3	2377	7.4	86.4	4.5	375	1.8	13.6	0.7
Southeast	112.5–157.5	8597	16.4	6990	21.9	81.3	13.4	1607	7.9	18.7	3.1
South	157.5–202.5	9534	18.2	8341	26.1	87.5	15.9	1193	5.9	12.5	2.3
Southwest	202.5–247.5	914	1.7	720	2.3	78.8	1.4	194	1.0	21.2	0.4
West	247.5–292.5	4988	9.5	2126	6.7	42.6	4.1	2862	14.0	57.4	5.5
Northwest	292.5–337.5	15112	28.9	5538	17.3	36.6	10.6	9574	47.0	63.4	18.3
6-h sustained wind forcing											
North	337.5–22.5	3149	13.6	1231	9.8	39.1	5.3	1918	18.0	60.9	8.3
Northeast	22.5–67.5	1552	6.7	1232	9.8	79.4	5.3	320	3.0	20.6	1.4
East	67.5–112.5	1091	4.7	1040	8.3	95.3	4.5	51	0.5	4.7	0.2
Southeast	112.5–157.5	2296	9.9	2027	16.2	88.3	8.7	269	2.5	11.7	1.2
South	157.5–202.5	4697	20.2	4260	34.0	90.7	18.4	437	4.1	9.3	1.9
Southwest	202.5–247.5	131	0.6	91	0.7	69.5	0.4	40	0.4	30.5	0.2
West	247.5–292.5	2468	10.6	735	5.9	29.8	3.2	1733	16.3	70.2	7.5
Northwest	292.5–337.5	7816	33.7	1921	15.3	24.6	8.3	5895	55.3	75.4	25.4
9-h sustained wind forcing											
North	337.5–22.5	1606	13.3	702	11.6	43.7	5.8	904	15.0	56.3	7.5
Northeast	22.5–67.5	744	6.2	644	10.6	86.6	5.3	100	1.7	13.4	0.8
East	67.5–112.5	487	4.0	485	8.0	99.6	4.0	2	0.0	0.4	0.0
Southeast	112.5–157.5	681	5.6	637	10.5	93.5	5.3	44	0.7	6.5	0.4
South	157.5–202.5	2582	21.4	2389	39.5	92.5	19.8	193	3.2	7.5	1.6
Southwest	202.5–247.5	14	0.1	9	0.1	64.3	0.1	5	0.1	35.7	0.0
West	247.5–292.5	1394	11.5	267	4.4	19.2	2.2	1127	18.7	80.8	9.3
Northwest	292.5–337.5	4562	37.8	917	15.2	20.1	7.6	3645	60.5	79.9	30.2
12-h sustained wind forcing											
North	337.5–22.5	870	12.8	477	14.8	54.8	7.0	393	11.1	45.2	5.8
Northeast	22.5–67.5	435	6.4	390	12.1	89.7	5.8	45	1.3	10.3	0.7
East	67.5–112.5	226	3.3	223	6.9	98.7	3.3	3	0.1	1.3	0.0
Southeast	112.5–157.5	252	3.7	247	7.6	98.0	3.6	5	0.1	2.0	0.1
South	157.5–202.5	1367	20.2	1248	38.6	91.3	18.4	119	3.4	8.7	1.8
Southwest	202.5–247.5	6	0.1	1	0.0	16.7	0.0	5	0.1	83.3	0.1
West	247.5–292.5	783	11.6	106	3.3	13.5	1.6	677	19.1	86.5	10.0
Northwest	292.5–337.5	2837	41.9	537	16.6	18.9	7.9	2300	64.8	81.1	33.9

interdepartmental communication, rapid-response mitigation practices, and notification to the public.

In addition to public safety concerns, local economic activity at City Dock has already been impacted by coastal nuisance flooding, and projections suggest that as little as 1 ft of RSL rise could reduce downtown visits by approximately 24% without further adaptation (Hino et al. 2019). Furthermore, reoccurring nuisance flooding is likely having a negative impact on coastal infrastructure including stormwater management systems and roadways (Sweet et al. 2014).

While these results can aid local stakeholders in mitigating against coastal nuisance flooding events, the analysis falls short of being a predictive tool for water levels or coastal nuisance flooding events. More comprehensive future studies should incorporate additional drivers of water level variability as they are likely important during instances of lower sustained wind forcing. These include, but are not limited to, precipitation and runoff, sea level pressure, water temperature variability in the Atlantic (e.g., Widlansky et al. 2020), river discharge (particularly the Susquehanna), and lower-amplitude and longer-duration processes. Future studies should consider techniques to better account for RSL rise and lagged WLA response, along with the application of more complex statistical approaches (e.g., machine learning approaches similar to Grbić et al. 2013) to model WLA response to variations in meteorological conditions and forcing. In addition, there is anecdotal evidence for a

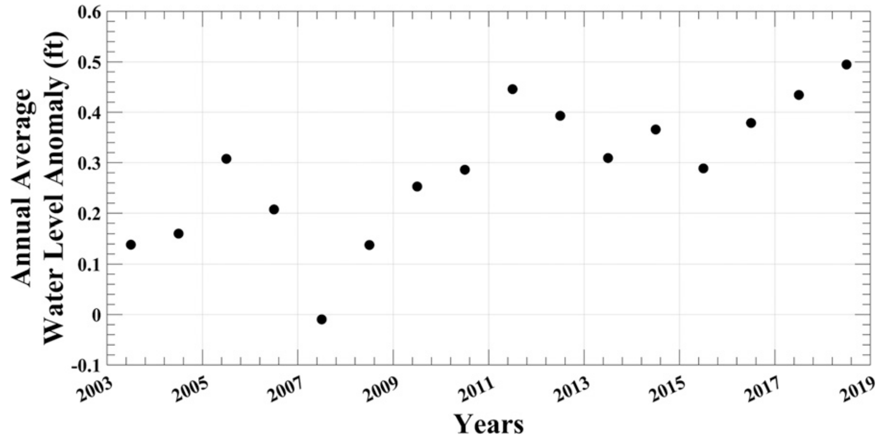

FIG. 7. Annual average water level anomaly in Annapolis from 2003 through 2019 (0.1 ft = 0.03 m).

nonlinear water level response in the Chesapeake Bay (and tributaries) associated with the relaxation of wind forcing that needs to be further investigated and accounted for.

5. Summary and conclusions

Like many coastal communities throughout the U.S. mid-Atlantic region, relative sea level rise and accelerating instances and duration of coastal nuisance flooding are having a tangible negative impact on economic activity and infrastructure in Annapolis, Maryland. Annapolis has experienced an exponential increase in hours above flood stage since the middle of the last century (Fig. 2) with over 2% of the most recent decade (2010–19) above flood stage. Coastal nuisance flooding is often the result of positive water level anomalies, which are a superposition of global, regional, and local influences that occur across spatial and temporal scales. Understanding short-duration water level variability is increasingly important as local stakeholders work to mitigate the impacts of coastal nuisance flooding.

In this study we focused specifically on the role of short-duration (hourly) sustained meteorological wind forcing on water level anomalies in Annapolis, Maryland, which is an ideal location to study these processes because of the orientation of the coast relative to the prevailing winds (Figs. 4 and 6). Our results suggest that positive water level anomalies occurred when the sustained directional wind forcing was out of the northeast, east, southeast, and south (Fig. 5), which corresponds to forcing into the mouth of the Severn River or up axis of the main stem of the Chesapeake Bay (Fig. 6). Meanwhile, negative water level anomalies occurred when the sustained directional wind forcing was out of the northwest and north (Fig. 5), which corresponds to wind forcing out of the Severn River and/or the Chesapeake Bay (Fig. 6). These relationships were the most coherent for longer duration wind forcing (6+ h) and higher wind speeds (15+ mph). However, higher sustained wind speeds over shorter durations likely also have an impact on water levels (Fig. 5a). We speculate that for low wind speeds over a shorter duration, wind forcing is a less relevant driver of water levels, or the signal is cluttered by the complexities of the estuarine coastal system.

Acknowledgments. This work was supported, in part, by the U.S. Defense Threat Reduction Agency (DTRA).

Data availability statement. All raw data used in this study are publicly accessible. Atmospheric data were downloaded

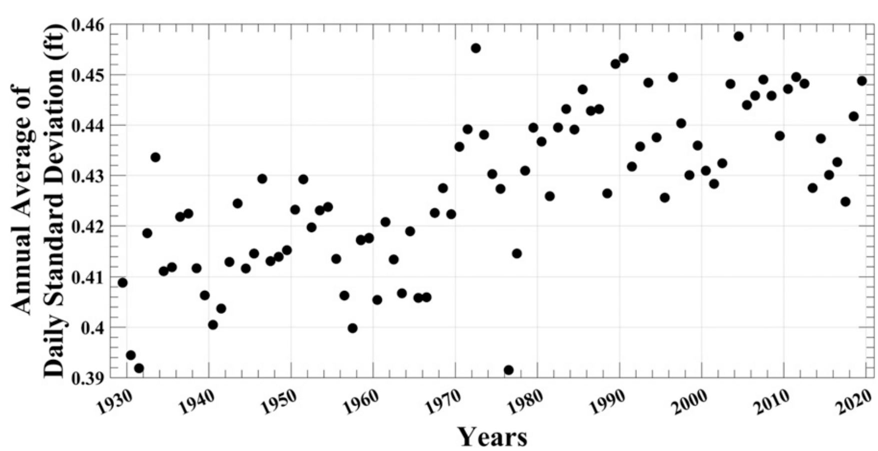

FIG. 8. Annual average of daily water level standard deviations in Annapolis (0.1 ft = 0.03 m).

from Iowa State University's Iowa Environmental Mesonet (https://mesonet.agron.iastate.edu/), but the atmospheric data are also publicly accessible through NOAA's National Centers for Environmental Information (https://www.ncei.noaa.gov/). Water level data and tidal predictions are publicly available through the NOAA National Ocean Service's Center for Operational Oceanographic Products and Services (https://tidesandcurrents.noaa.gov/). All data required to make Fig. 5 are available in Table 1. Data specifically downloaded for this study will be made available upon request.

REFERENCES

Anne Arundel County, 2020: Severn River Commission. Anne Arundel County, Maryland, accessed 2 May 2021, https://www.aacounty.org/boards-and-commissions/severn-river-commission/index.html.

Boon, J. D., 2012: Evidence of sea level acceleration at U.S. and Canadian tide stations, Atlantic Coast, North America. *J. Coastal Res.*, **28**, 1437–1445, https://doi.org/10.2112/JCOASTRES-D-12-00102.1.

——, J. M.Brubaker, and D. M.Forrest, 2010: Chesapeake Bay Land subsidence and sea level change: An evaluation of past and present trends and future outlook. Virginia Institute of Marine Science Applied Marine Science and Ocean Engineering Special Rep. 425, 81 pp., https://doi.org/10.21220/V58X4P.

Cazenave, A., and G.Le Cozannet, 2013: Sea level rise and its coastal impacts. *Earth's Future*, **2**, 15–34, https://doi.org/10.1002/2013EF000188.

Church, J. A., and N. J. White, 2011: Sea-level rise from the late 19th to the early 21st century. *Surv. Geophys.*, **32**, 585–602, https://doi.org/10.1007/s10712-011-9119-1.

Cox, D., P. Tissot, and P. Michaud, 2002: Water level observations and short-term predictions including meteorological events for entrance of Galveston Bay, Texas. *J. Waterw. Port Coastal Ocean Eng.*, **128**, 21–29, https://doi.org/10.1061/(ASCE)0733-950X(2002)128:1(21).

Dahl, K. A., M. F. Fitzpatrick, and E. Spanger-Siegfried, 2017: Sea level rise drives increased tidal flooding frequency at tide gauges along the U.S. East and Gulf Coasts: Projections for 2030 and 2045. *PLOS ONE*, **12**, e0170949, https://doi.org/10.1371/journal.pone.0170949.

Eggleston, J., and J. Pope, 2013: Land subsidence and relative sea-level rise in the southern Chesapeake Bay region. U.S. Geological Survey Circular 1392, 30 pp., https://doi.org/10.3133/cir1392.

Ezer, T., 2015: Detecting changes in the transport of the Gulf Stream and the Atlantic overturning circulation from coastal sea level data: The extreme decline in 2009–2010 and estimated variation for 1935–2012. *Global Planet. Change*, **129**, 23–36, https://doi.org/10.1016/j.gloplacha.2015.03.002.

——, 2019: Regional difference in sea level rise between the mid-Atlantic Bight and the south Atlantic Bight: Is the Gulf Stream to blame?*Earth's Future*, **7**, 771–783, https://doi.org/10.1029/2019EF001174.

——, and L. P. Atkinson, 2014: Accelerated flooding along the U.S. East Coast: On the impact of sea-level rise, tides, storms, the Gulf Stream, and the North Atlantic Oscillations. *Earth's Future*, **2**, 362–382, https://doi.org/10.1002/2014EF000252.

——, ——, W. B. Corlett, and J. L. Blanco, 2013: Gulf Stream's induced sea level rise and variability along the U.S. mid-Atlantic coast. *J. Geophys. Res. Oceans*, **118**, 685–697, https://doi.org/10.1002/jgrc.20091.

Flick, R. E., J. F. Murray, and L. C. Ewing, 2003: Trends in United States tidal datum statistics and tide range. *J. Waterw. Port Coastal Ocean Eng.*, **155**, 155–164, https://doi.org/10.1061/(ASCE)0733-950X(2003)129:4(155).

Fujita, T. T., 1981: Tornadoes and downbursts in the context of generalized planetary scales. *J. Atmos. Sci.*, **38**, 1511–1534, https://doi.org/10.1175/1520-0469(1981)038<1511:TADITC>2.0.CO;2.

Ganguli, P., and B. Merz, 2019: Extreme coastal water levels exacerbate fluvial flood hazards in northwestern Europe. *Sci. Rep.*, **9**, 13165, https://doi.org/10.1038/s41598-019-49822-6.

Grbić, R., D. Kurtagić, and D. Slišković, 2013: Stream water temperature prediction based on Gaussian process regression. *Expert Syst. Appl.*, **40**, 7407–7414, https://doi.org/10.1016/j.eswa.2013.06.077.

Gregory, J. M., and Coauthors, 2013: Twentieth-century global-mean sea level rise: Is the whole greater than the sum of the parts?*J. Climate*, **26**, 4476–4499, https://doi.org/10.1175/JCLI-D-12-00319.1.

Hall, J. A., S. Gill, J. Obeysekera, W. Sweet, K. Knuuti, and J. Marburger, 2016: Regional sea level scenarios for coastal risk management: Managing the uncertainty of future sea level change and extreme water levels for department of defense coastal sites worldwide. U.S. Department of Defense, Strategic Environmental Research and Development Program Rep., 224 pp., https://apps.dtic.mil/sti/pdfs/AD1013613.pdf.

Hicks, S. D., R. L. Sillcox, C. R. Nichols, B. Via, and E. C. McCray, 2000: Tide and current glossary. NOAA/National Ocean Service Doc., 33 pp., https://tidesandcurrents.noaa.gov/publications/glossary2.pdf.

Hino, M., S. T. Belanger, C. B. Field, A. R. Davies, and K. J. Mach, 2019: High-tide flooding disrupts local economic activity. *Sci. Adv.*, **5**, eaau2736, https://doi.org/10.1126/sciadv.aau2736.

Kemp, A. C., and B. P. Horton, 2013: Contribution of relative sea-level rise to historical hurricane flooding in New York City. *J. Quat. Sci.*, **28**, 537–541, https://doi.org/10.1002/jqs.2653.

Kopp, R. E., 2013: Does the mid-Atlantic United States sea level rise acceleration hot spot reflect ocean dynamic variability?-*Geophys. Res. Lett.*, **40**, 3981–3985, https://doi.org/10.1002/grl.50781.

——, C. C. Hay, C. M. Little, and J. X. Mitrovica, 2015: Geographic variability of sea-level change. *Curr. Climate Change Rep.*, **1**, 192–204, https://doi.org/10.7282/T37W6F4P.

Lyddon, C., J. M. Brown, N. Leonardi, and A. J. Plater, 2018: Uncertainty in estuarine extreme water level predictions due to surge-tide interaction. *PLOS ONE*, **13**, e0206200, https://doi.org/10.1371/journal.pone.0206200.

Markowski, P., and Y. Richardson, 2010: *Mesoscale Meteorology in Midlatitude*. John Wiley and Sons, 407 pp.

McInnes, K. L., G. D. Hubbert, D. J. Abbs, and S. E. Oliver, 2002: A numerical modelling study of coastal flooding. *Meteor. Atmos. Phys.*, **80**, 217–233, https://doi.org/10.1007/s007030200027.

Merrifield, M. A., S. T. Merrifield, and G. T. Mitchum, 2009: An anomalous recent acceleration of global sea level rise. *J. Climate*, **22**, 5772–5781, https://doi.org/10.1175/2009JCLI2985.1.

Miller, K. G., R. E. Kopp, B. P. Horton, J. V. Browning, and A. C. Kemp, 2013: A geological perspective on sea-level rise and its impact along the U.S. mid-Atlantic coast. *Earth's Future*, **1**, 3–18, https://doi.org/10.1002/2013EF000135.

Morris, J. T., and K. A. Renken, 2020: Past, present, and future nuisance flooding on the Charleston peninsula. *PLOS ONE*, **15**, e0238770, https://doi.org/10.1371/journal.pone.0238770.

NOAA, 2020: Environmental measurement systems—Sensor specifications and measurement algorithm. Center for Operational Oceanographic Products and Service, accessed 29 September 2021, https://tidesandcurrents.noaa.gov/publications/CO-OPS_Measurement_Spec.pdf.

——, 2021: Advanced hydrological prediction service—Severn River forecast at Annapolis. Accessed 23 September 2021, https://water.weather.gov/ahps2/hydrograph.php?gage=apam2&wfo=lwx.

Orlanksi, I., 1975: A rational subdivision of scales for atmospheric processes. *Bull. Amer. Meteor. Soc.*, **56**, 527–530, https://doi.org/10.1175/1520-0477-56.5.527.

Parris, A., and Coauthors, 2012: Global sea level rise scenarios for the United States: National Climate Assessment. NOAA Tech. Memo. OAR CPO-1, 33 pp., https://scenarios.globalchange.gov/sites/default/files/NOAA_SLR_r3_0.pdf.

Sallenger, A., K. Doran, and P. Howd, 2012: Hotspot of accelerated sea-level rise on the Atlantic coast of North America. *Nat. Climate Change*, **2**, 884–888, https://doi.org/10.1038/nclimate1597.

Serafin, K. A., P. Ruggiero, and H. F. Stockdon, 2017: The relative contribution of waves, tides, and nontidal residuals to extreme total water levels on U.S. West Coast sandy beaches. *Geophys. Res. Lett.*, **44**, 1839–1847, https://doi.org/10.1002/2016GL071020.

Sheridan, S. C., D. E. Douglas, E. Pirhalla, C. C. Lee, and V. Ransibrahmanakul, 2017: Atmospheric drivers of sea-level fluctuations and nuisance floods along the mid-Atlantic coast of the USA. *Reg. Environ. Change*, **17**, 1853–1861, https://doi.org/10.1007/s10113-017-1156-y.

Smeed, D. A., and Coauthors, 2014: Observed decline of the Atlantic meridional overturning circulation 2004–2012. *Ocean Sci.*, **10**, 29–38, https://doi.org/10.5194/os-10-29-2014.

Srokosz, M., M. Baringer, H. Bryden, S. Cunningham, T. Delworth, S. Lozier, J. Marotzke, and R. Sutton, 2012: Past, present, and future change in the Atlantic meridional overturning circulation. *Bull. Amer. Meteor. Soc.*, **93**, 1663–1676, https://doi.org/10.1175/BAMS-D-11-00151.1.

Sweet, W. V., and C. Zervas, 2011: Cool-season sea level anomalies and storm surges along the U.S. East Coast: Climatology and comparison with the 2009/10 El Niño. *Mon. Wea. Rev.*, **139**, 2290–2299, https://doi.org/10.1175/MWR-D-10-05043.1.

——, and J. Park, 2014: From the extreme to the mean: Acceleration and tipping points of coastal inundation from sea level rise. *Earth's Future*, **2**, 579–600, https://doi.org/10.1002/2014EF000272.

——, C. Zervas, and S. Gill, 2009: Elevated East Coast sea level anomaly: July–July 2009. NOAA Tech. Rep. NOS CO-OPS-051, 40 pp., https://tidesandcurrents.noaa.gov/publications/EastCoastSeaLevelAnomaly_2009.pdf.

——, J. Park, J. J. Marra, C. Zervas, and S. Gill, 2014: Sea level rise and nuisance flood frequency changes around the United States. NOAA Tech. Rep. NOS CO-OPS-073, 58 pp., https://doi.org/10.13140/2.1.3900.2887.

Thompson, P. R., G. T. Mitchum, C. Vonesch, and J. Li, 2013: Variability of winter storminess in the eastern United States during the twentieth century from tide gauges. *J. Climate*, **26**, 9713–9726, https://doi.org/10.1175/JCLI-D-12-00561.1.

Widlansky, M. J., X. Long, and F. Schloesser, 2020: Increase in sea level variability with ocean warming associated with the nonlinear thermal expansion of seawater. *Commun. Earth Environ.*, **1**, 9, https://doi.org/10.1038/s43247-020-0008-8.

Wolf, J., 2009: Coastal flooding: Impacts of coupled wave-surge-tide models. *Nat. Hazards*, **49**, 241–260, https://doi.org/10.1007/s11069-008-9316-5.

Zervas, C., S. Gill, and W. V. Sweet, 2013: Estimating vertical land motion from long-term tide gauge records. NOAA Tech. Rep. NOS CO-OPS-065, 22 pp., https://doi.org/10.25607/OBP-141.

Zhang, K., and B. C. Douglas, 2000: Twentieth-century storm activity along the U.S. East Coast. *J. Climate*, **13**, 1748–1761, https://doi.org/10.1175/1520-0442(2000)013<1748:TCSAAT>2.0.CO;2.